LAWRENCE
LIVERMORE
NATIONAL
LABORATORY

LLNL-TR-409726

LIFE Materials: Topical Assessment Report for LIFE Volume 1 TOPIC: Solid First Wall and Structural Components TASK: Radiation Effects on First Wall

A. Caro

January 8, 2009

Disclaimer

This work performed under the auspices of the U.S. Department of Energy by Lawrence Livermore National Laboratory under Contract DE-AC52-07NA27344.

LIFE Materials:

Topical Assessment Report for LIFE

Volume 1

TOPIC: **Solid First Wall and Structural Components**
TASK: **Radiation Effects on First Wall.**

Part II: Steel component

Alfredo Caro

With contributions from the Materials Science Team: M. Caro, J. Marian, M. Fluss, P DeMange, and L. Zepeda-Ruiz

July 8, 2008

The present document discusses relevant radiation damage issues affecting the first wall of LIFE. We explore the use of ODS ferritic steels for the wall from the perspective of mechanical properties and radiation damage

This work was performed under the auspices of the U.S. Department of Energy by Lawrence Livermore National Laboratory under Contract DE-AC52-07NA27344.

Table of content:

CHAPTER A: LIFE Requirements for Materials. Part II: The structure of the First Wall

The problem: As discussed in Part I (Tungsten coating) of this First Wall Topical report, the fusion energy generated in the target is carried away by different forms of radiation, namely neutrons, ions, gammas, and X-rays. Only neutrons penetrate into the Fe component of the wall, the other forms of radiation being stopped at the W armor. Neutron damage is the main concern for this component and is the determining factor of its lifetime. Additionally, because the first wall, FW, faces the 14 MeV fusion neutron source closer than any other component, the hardness of the spectrum it receives is such that He and H produced by transmutation are the major source of damage.

Basic requirements: Fusion and advanced fission energy will require new high performance structural alloys with outstanding properties that are sustained under long term service in severe environments, including neutron damage in the range of 100's of dpa and He production in the range of 1000's atomic parts per million, appm.

The LIFE engine is assumed to consist of a 2.25 m radius spherical fusion chamber filled with argon. The first wall consists of 500 microns of a tungsten armor on a 3 mm iron substrate. The base temperature for these materials is 873K.

In Part I we discussed the thermal cycling of the FW and concluded that temperature oscillations due to the pulsed nature of the source only affect the first few 100's microns of the W armor. The structural part of the FW sees a constant T environment. Therefore basic requirements for a FW in a fusion-fission device are:

i- Good thermal conductivity to carry the heat towards the coolant,

ii- Irradiation damage resistance to provide a long lifetime with properties unchanged

iii- High tensile, creep and fatigue strength to act as structural material.

iv- High swelling and embrittlement resistance in the presence of large amounts of He.

Base-line material's properties: The requirements listed above determine what the materials options are. Fusion devices place constraints on materials that are at the limit of

present day technology. Figure 1 shows a schematic view of the specifications that clearly shows the extreme damage doses and temperatures.

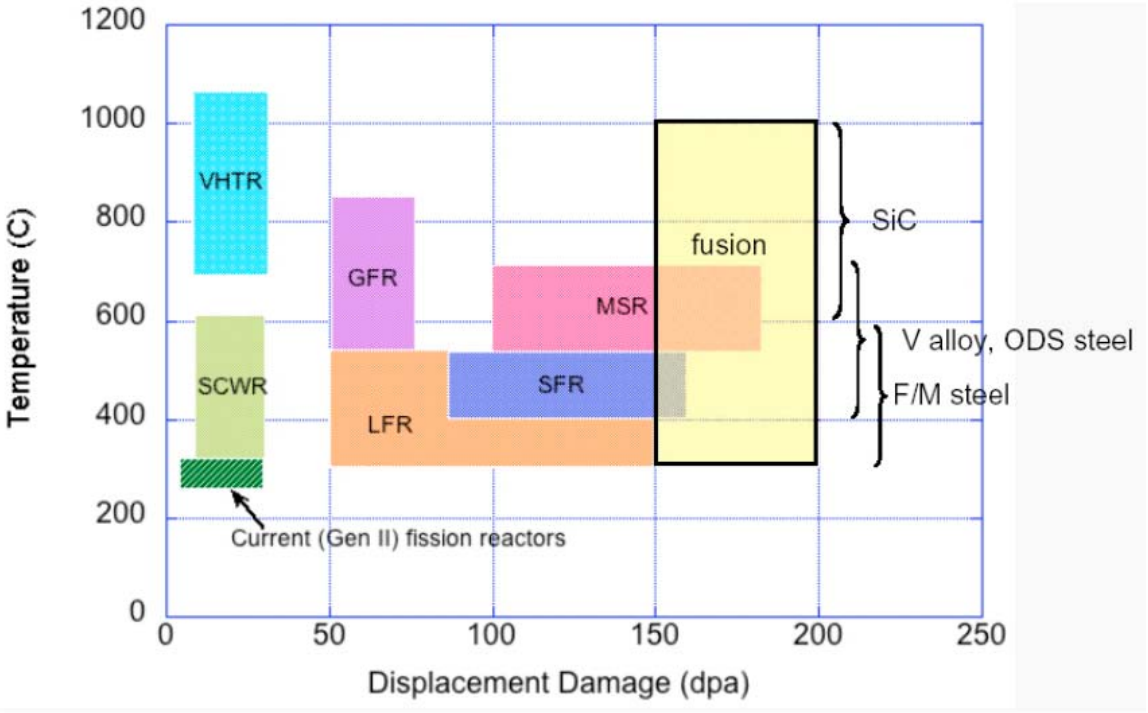

Figure 1: Operating temperature and damage doses for different nuclear concepts. Clearly Gen IV and fusion reactors pose severe materials challenges. From S. Zinkle ORNL.

From the discussion in Part I, the preferred first wall configuration to consider is tungsten-coated nanostructured ferritic steel. Also in Part I we saw that the requirement of low activation steel formulations present in the FW for Magnetic Fusion Energy, MFE, is not present in this case, enlarging the options available. Nonetheless a strong difference between IFE and MFE is the damage rate, since for an equal total fusion energy, the pulsed nature of IFE makes the instantaneous neutron displacement rate, dpa-rate, about 10 dpa/sec compared to 10^{-6} dpa/sec for MFE. Damage rate effects are very difficult to assess from modeling and experimental perspectives today and therefore present a particular challenge for LIFE.

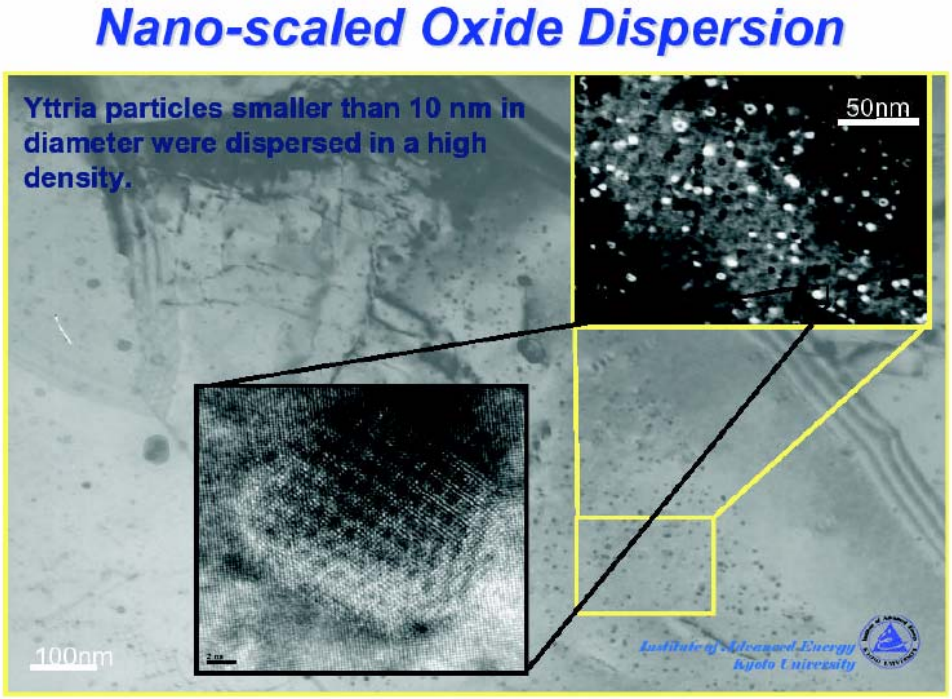

Figure 2: Picture of the structure of a ODS steel showing the high density of nanometer scale precipitates. From (xx) Kimura et al, 2006.

The candidate materials: ODS, or Oxide dispersion strengthened ferritic steels, is a new class of materials with an ultra high density of nanosclae Y-Ti-O particles that along with fine grains and high dislocation densities provide remarkable properties. These materials are under development at several places around the world, and long irradiation experiments are being conducted to understand their radiation stability. The oxide particles provide sites acting as sinks for defects produced by irradiation. They also provide dislocation pinning centers that improve the mechanical strength. Figure 2 shows the very high density of nanoparticles.

Nb-Zr and V alloys are alternative options for the first wall that we do not address in this report.

A qualitative view of the challenge: The high burn up proposed in LIFE, the damage by displacements and the production of He and H places LIFE materials

requirements at extreme conditions, some of them beyond the present day limits. For some particular configurations of LIFE, such as a burner of HEU or Pu, the requirements are within reach of an R&D plan in a short time, while other applications require more R&D effort.

Schematically, Figure 3 shows today's limits together with LIFE objectives. The two red circles LEU and HEU indicate present day experience with reactors burning low and highly enriched uranium respectively. Both cases correspond to thermal spectrum and are so indicted in the x-axis reporting the He and H per dpa rate, low values corresponding to thermal spectrum and high values to fast spectrum. In the burn up y-axis, LEU is typically burned up to about 10% Fraction of Initial Metal Atom, FIMA, while HEU and Pu have been burned up to ~ 80% FIMA. On the fluence / dpa z-axis, both LEU and HEU reach their limit at about 10^{21} n/cm^2. The horizontal plane at z= ~10^{21} n/cm^2 indicates the limit for structural/cladding material resistance. The vertical plane indicates the LIFE parametric space; with a spectrum that is a mixture of thermal plus the strong 14 MeV component, the He-H/dpa is situated midrange between a fast and thermal reactor, at about 20 He/dpa at the first wall. The vertical plane extends to 99 % FIMA and on it we plotted an ellipse that shows the fluence needed to burn HEU or PU (lowe fluence) and to burn LEU or DU (high fluence). The green arrows indicate the path that is necessary to follow to go from present day possibilities to LIFE objectives. Clearly to go from 80 to 99% FIMA in HEU or Pu the distance in this parametric space is short, while to go from 10 to 99 % FIMA in LEU or DU there is a major challenge.

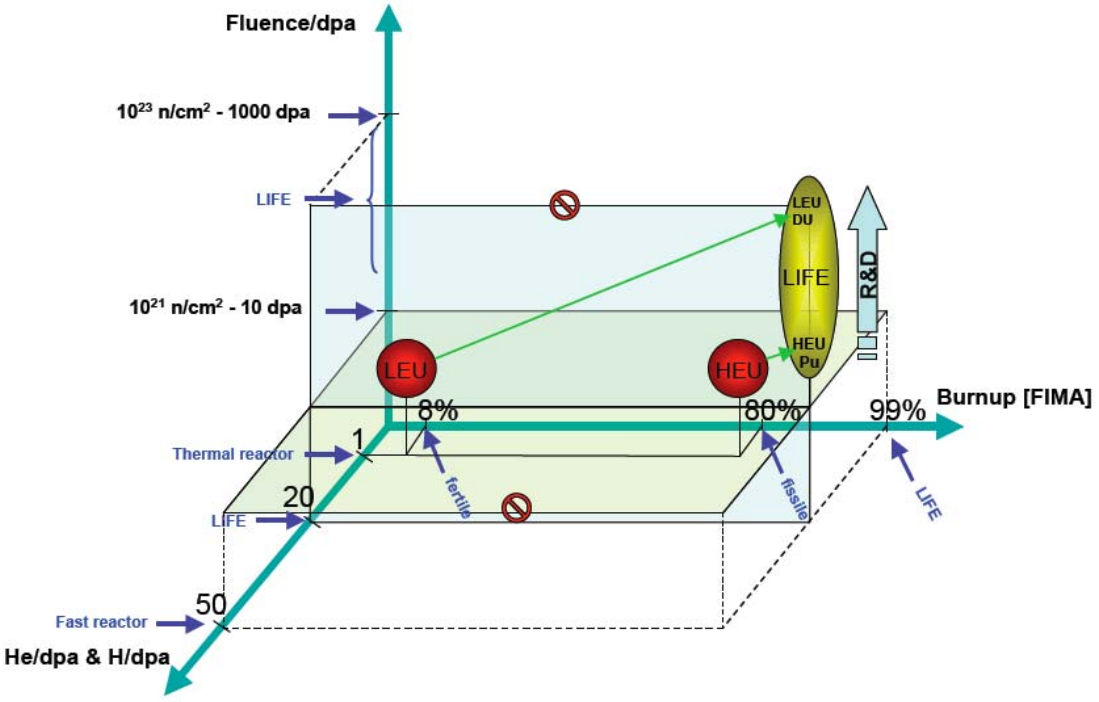

Figure 3: Schematic representation of the parameter space of different LIFE objectives. The mixed spectrum of LIFE places it at a mid range in He/dpa and H/dpa production. The high burn up objective places LIFE at the extreme of the present day experience. The fluences needed to reach the two objectives, burning LEU or HEU are significantly different. The green arrows indicate the distance to cover from today's possibilities to LIFE goals.

CHAPTER B: Summary of Existing Knowledge

Brief historical introduction: In this section we briefly summarize previous and ongoing efforts to develop irradiation damage resistant alloys, following the lines of a recent review by Odette et al 2008 (1).

Steels for nuclear application are classified as austenitic (based on the fcc phase of Fe,) and ferritic (based on the bcc phase of Fe). Swelling-resistant cold-worked austenitic stainless steels containing stable, fine-scale M(Ti)C and phosphide precipitates both trap He and provide stable, sink-dominated microstructures that promote point defect recombination to resist various adverse effects of irradiation, including void swelling. These alloying/processing changes also avoid the coarse radiation-induced phases that directly or indirectly promote void formation by the control of microalloying elements like B, P, Si, and carbide formers like Ti, Nb and/or V. These advanced austenitic stainless steels also have the added benefit of high creep resistance arising from their stable fine-scale precipitate microstructures that pin dislocations. For a few papers representing the much larger literature on this subject, see References (2–4).

Ferritic alloys are even more swelling resistant than the advanced austenitic alloys, especially at lower He levels and He/dpa ratios. Responsible mechanisms include the bcc structure, with a smaller dislocation bias and a higher self-diffusion coefficient, lower He concentrations in the absence of Ni (thermal neutrons transmute Ni to He), high sink densities, and nanoscale distributions of bubbles that form on dislocations in submicrometer lath structures, thereby also retarding coarsening (5, 6).

Recently, Klueh and coworkers at Oak Ridge National Laboratory (6, 7) have developed new microalloyed and/or specially processed 9Cr ferritic / martensitic with much higher creep strength compared with conventional 9Cr alloys, for possible use up to 700◦C. High creep strength requires properly balancing the alloy composition (N, C, B, Ti, Ta, V, Nb) coupled with thermal mechanical treatments (TMTs) to form stable, nanoscale precipitates. In this case, the precipitates, which also provide much of the strength in conventional 9Cr TMS, are approximately four times smaller (7–8 nm) at

number densities of up three orders of magnitude higher (2-9 10^{21} m^{-3}). Refinement of the nanoscale phases results from a combination of N additions and warm working to provide abundant heterogeneous precipitation sites on dislocations.

Although the pertinent data of these steels are limited, these materials also appear to have the stable nano-microstructural attributes required for irradiation damage resistance. However, even the most advanced stainless steels have the potential eventually to swell at high rates when their protective microstructures break down at large doses, and they can manifest poor mechanical properties owing to the formation of embrittling radiation-induced features at lower temperatures, and grain boundary He embrittlement at high temperatures. The detailed performance of these alloys at high He levels is not well known. Certainly more data at high end-of-life doses are needed to address these concerns.

Nano-structured ferritic alloys, NFA, are 12–20% Cr ferritic stainless steels that are dispersion strengthened by a very high density of ultrafine Y-Ti-O-enriched nanofeatures. Their roots trace to the pioneering work of Fisher, who patented a mechanical alloying (MA)/hot extrusion powder processing route to produce NFAs, which were marketed in the 1980s as International Nickel Company (INCO) MA956 and MA957 (8). The high Al content in MA956 and Plansee PM2000 results in somewhat coarser features and lower strength (9). Extensive studies in the U.S. breeder reactor program showed that MA957 has high tensile strength and creep strength as well as unusual resistance to radiation damage (10).

Research on nano-dispersion-strengthened alloys in Japan culminated in the successful development of dual-phase 9Cr nanostructured transformable steels, NTS, for fast-reactor-fuel cladding, as described in a recent review paper (11). The Japanese program placed special emphasis on working-recrystallization sequences that are necessary for plate and tubing fabrication and that also produce more isotropic properties. This processing research was complemented by evaluations of irradiation responses (12-27).

In Europe, various processing and characterization studies were performed on MA957 and small experimental heats of NFAs (28–33). More recently, European

research has been aimed at developing the martensitic ODS Eurofer97 for fusion applications (34-46).

U.S. research has focused on NFAs (47-67), including their response to irradiation (68–73). NFAs alloyed with small amounts of Ti, are now known to contain a high density of NFs enriched in Y-Ti-O. NFAs have fine-grain sizes and moderate-to-high dislocation densities, resulting in high tensile and creep strengths. This is illustrated in Figure 4, which shows a creep rupture time (t_r) Larson-Miller plot for a Japanese NFA, J12YWT (59), and a 9Cr TMS Eurofer97 (74). The insets show an atom probe tomography (APT) map and Y-Ti-O cluster image for the NFs in J12YWT (51), along with the average radius (r), number density (N), and volume fraction (f), measured by small-angle neutron scattering (SANS) (53, 55, 58). These ultrafine-scale features distinguish NFAs from conventional dispersion strengthened ODS alloys, which generally contain refined, but larger, equilibrium oxide phases.

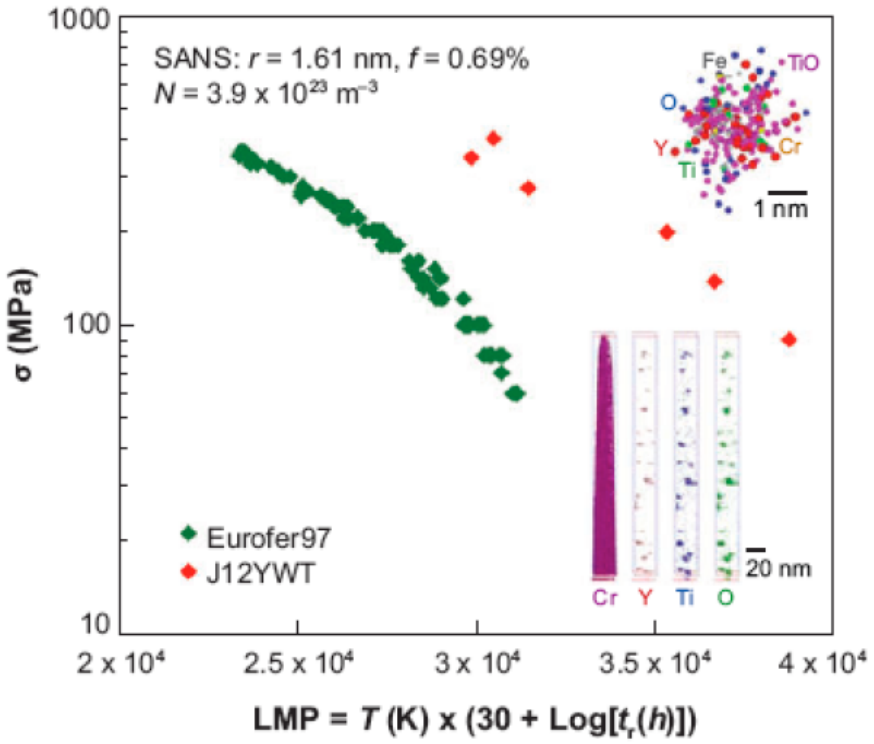

Figure 4: A Larson-Miller plot (LMP) comparing the creep strength of nanostructured ferritic alloys J12YWT (59) with that of normalized and tempered martensitic steel Eurofer97 (74). The insets show atom probe tomography maps of the

nanofeatures (NF) in J12YWT (51). Small-angle neutron scattering (SANS) data on the NF size (r), number density (N), and volume fraction (f) are shown (top left) (55, 58).

From this ensemble of work we extracted the information neded ofr our study, that we present in what follows, classified by issues or metallurgical variables.

Design window: Radiation damage affects several properties of materials that taken together define the design window for the particular application. Figure 5 shows as an example such a window for Nb1Zr alloys (75). In the tensile strength axes, 1/3 of the ultimate tensile stress (UTS) is taken as upper limit for safety considerations. In the temperature axis, low temperature introduces embrittlement, as bcc alloys show a ductile to brittle transition whose transition temperture increase with irradiation. On the high T boundary, thermal and radiation induced creep rupture limits the window.

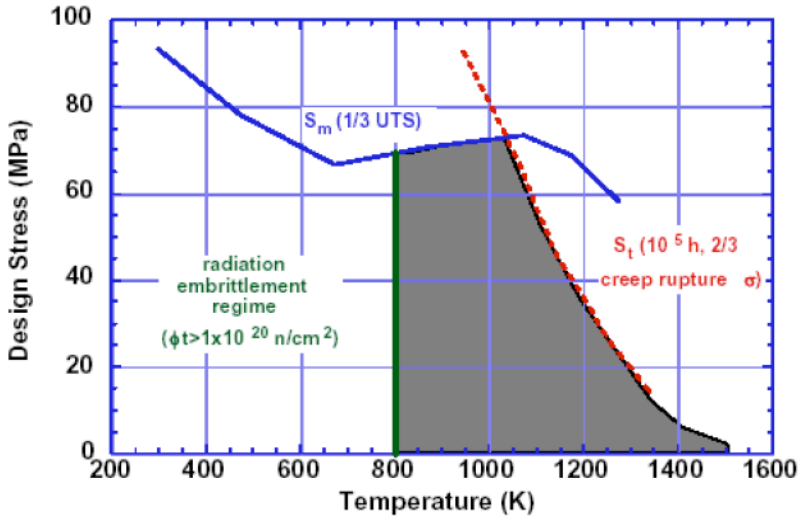

Figure 5: Material properties define the design window for nuclear applications. Example showing the case for Nb 1Zr. From S. Zinkle (75).

The temperature window: In service, components of a nuclear plant may undergo temperature changes due to transients, accidents, and start/stop operations. Curiously enough, all materials used in nuclear applications show a similar T-window of approximately 300 C, regardless of the absolute value of the operation T range, see Figure 6, from (75).

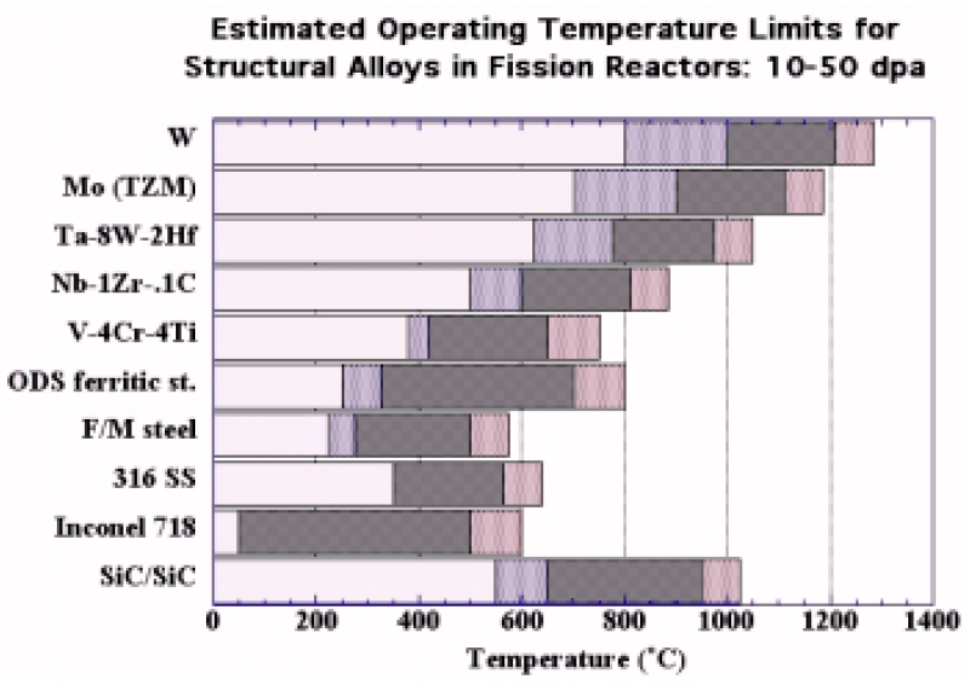

***Figure 6**: Operating temperature windows for various classes of reactor materials. The upper and lower bands are temperature ranges where the materials performance may be adequate, but insufficient data currently exists to confirm performance. From S. Zikle (75).*

Evolution of the design window with damage: Critical for the design of a nuclear component is that the design window evolves with irradiation dose. Figure 7 schematically shows the evolution of the boundaries. The tensile strength incases under irradiation, but the evolution of the other two boundaries makes this strengthening property of not use: Radiation damage increases the ductile to brittle transition temperature, DBTT, and decreases the creep resistance in a way that the are of the window in the parameter space shrinks as a function of dose.

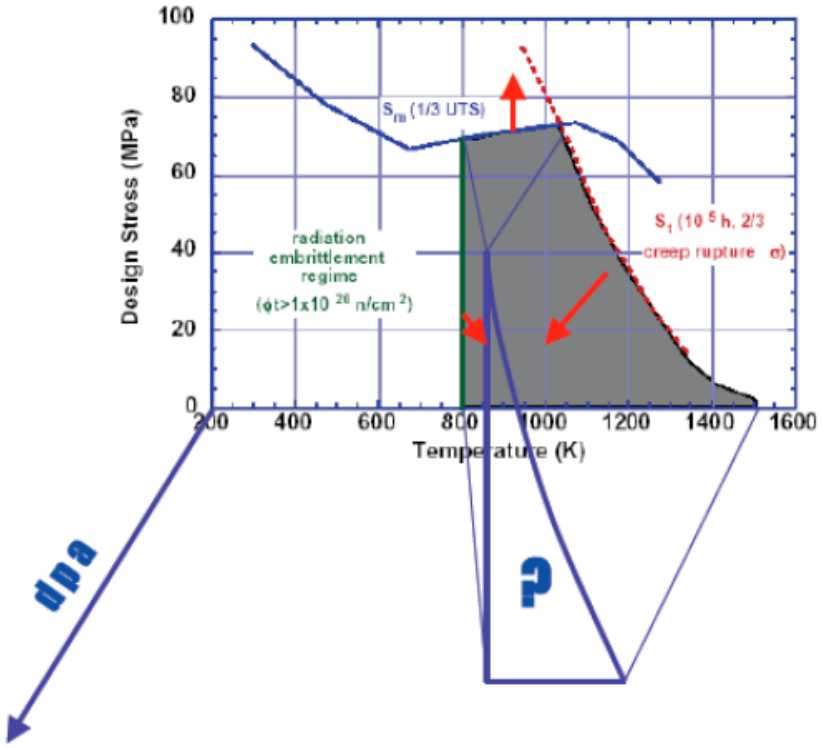

Figure 7: The design window evolves with radiation dose, reducing the range of stress and temperature where the given material can be used.

Damage calculations: The dpa damage is basically the result of the multiplication of the neutron spectrum times the dpa cross-section. This cross-section mainly reflects the linear damage model of Kinchin and Pease stating that the damage energy divided by the amount of energy to create a displacement gives the number of displaced atoms. The damage energy is mainly the kinetic energy of the neutron modified by the possible nuclear reactions [n,x], producing recoil transmutants with their own damage kinetic energy. For low neutron energies, below the displacement energy, typically a few eV, the dpa cross-section shows a linear (in a log-log plot) increase with decreasing energy, reflecting the n-capture process. Figure 8 shows the dpa cross-section for Fe and a typical spectrum for LIFE (case xx).

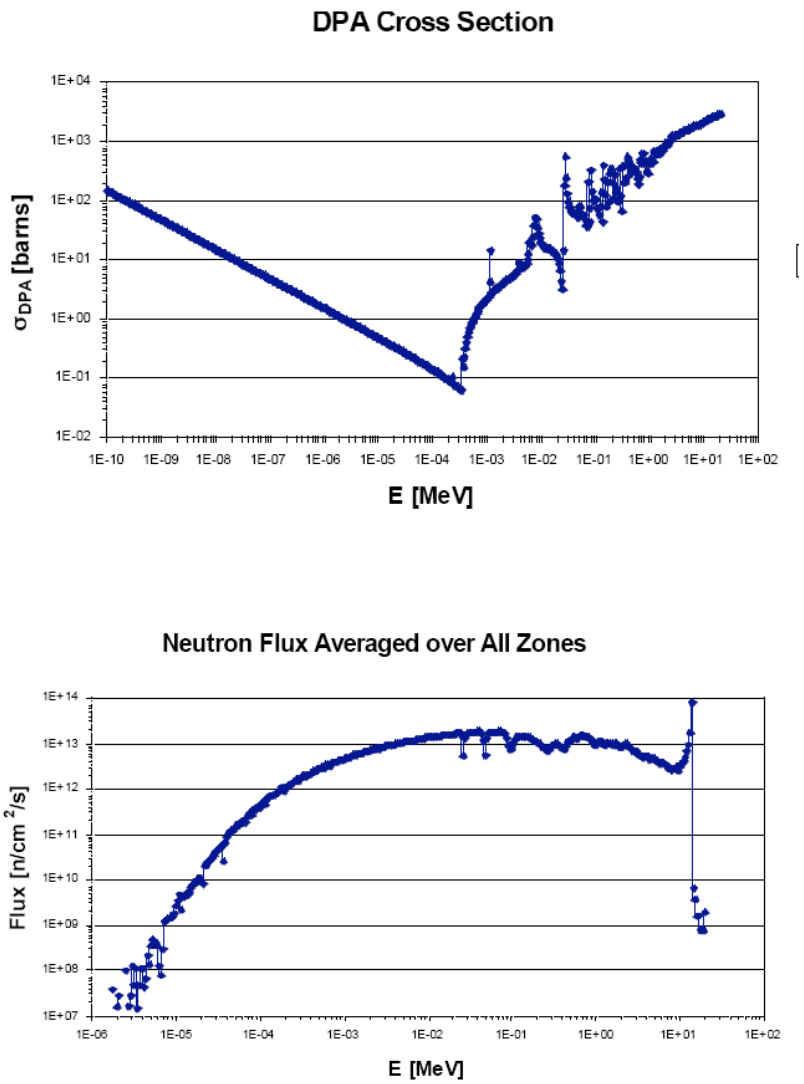

Figure 8: the Fe dpa cross section from Specter (upper figure), and the LIFE neutron spectrum averaged over the entire blanket, case (xx) (lower figure).

He and H production: One of the major factors affecting the material properties is the presence of fission gasses, H and He. H form brittle hydrides that enhance intergranular embrittlement and He is insoluble in Fe, forming bubbles and therefore leading to swelling. For fast neutron spectra, as those characteristic of fusion plants, the transmutation of Fe into H and He has a much greater cross section because these are threshold reaction. Figure 9 shows the nuclear cross section for Fe56 [n,α] and Fe56 [n,p] channels from ENDF http://www.nndc.bnl.gov/exfor/endf00.htm.

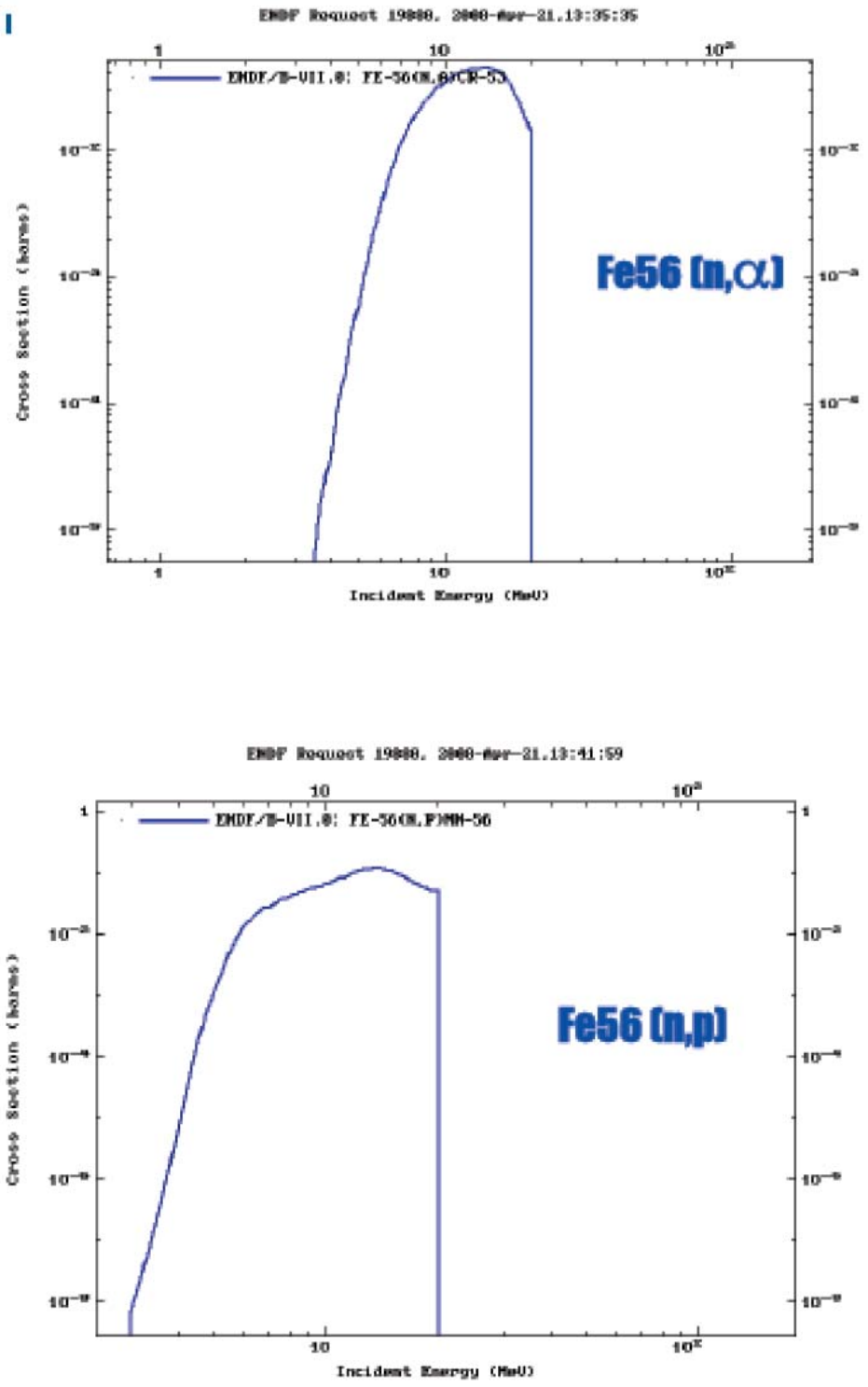

Figure 6: Nuclear cross sections for Fe56 [n,α] and Fe56 [n,p] chnnels. Note the thresholds of ~ 3.5 MeV for [n,α] and ~ 1.5 MeV for [n,p]. From http://www.nndc.bnl.gov/exfor/endf00.htm.

Swelling resistance: As already mentioned, ferritic steels have a bcc crystal structure that, in contrast to the fcc structure found in austenitic stainless steels, are more swelling resistant than the advanced austenitic alloys, especially at lower He levels and He/dpa ratios. The difference is substantial, as shown in Figure 7.

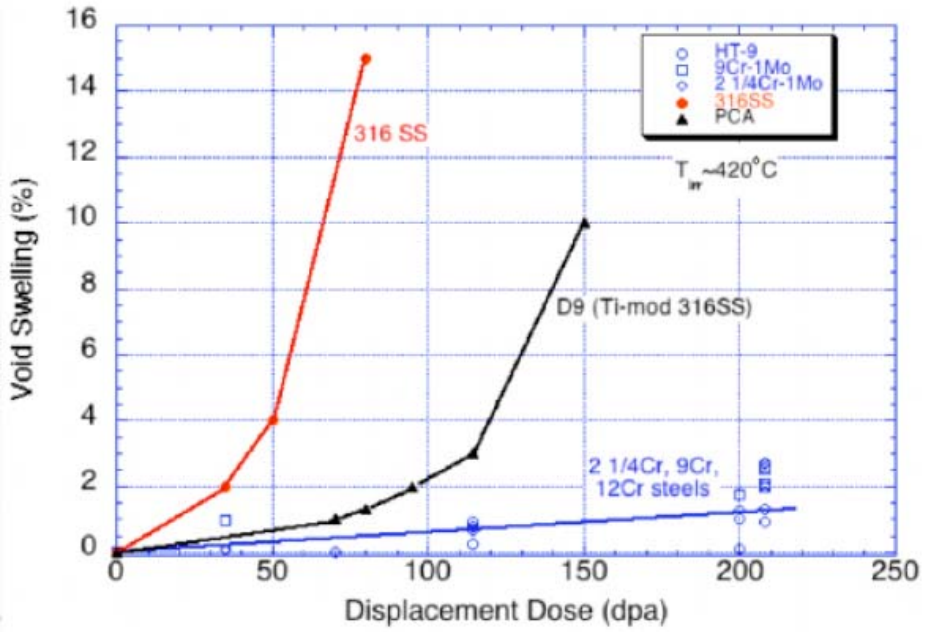

Figure 7: Void swelling as a function of dose in dpa for two austenitic and on ferritic steels. Clearly the welling resistance of ferritic steels is superior. From (76).

The responsible mechanisms for this difference are diverse, including the bcc structure itself, with a smaller dislocation bias for self interstitial trapping and a higher self-diffusion coefficient, lower He concentrations in the absence of Ni (thermal neutrons transmute Ni to He), high sink densities, and nanoscale distributions of bubbles that form on dislocations in sub-micrometer lath structures, thereby also retarding coarsening (79, 5, 6).

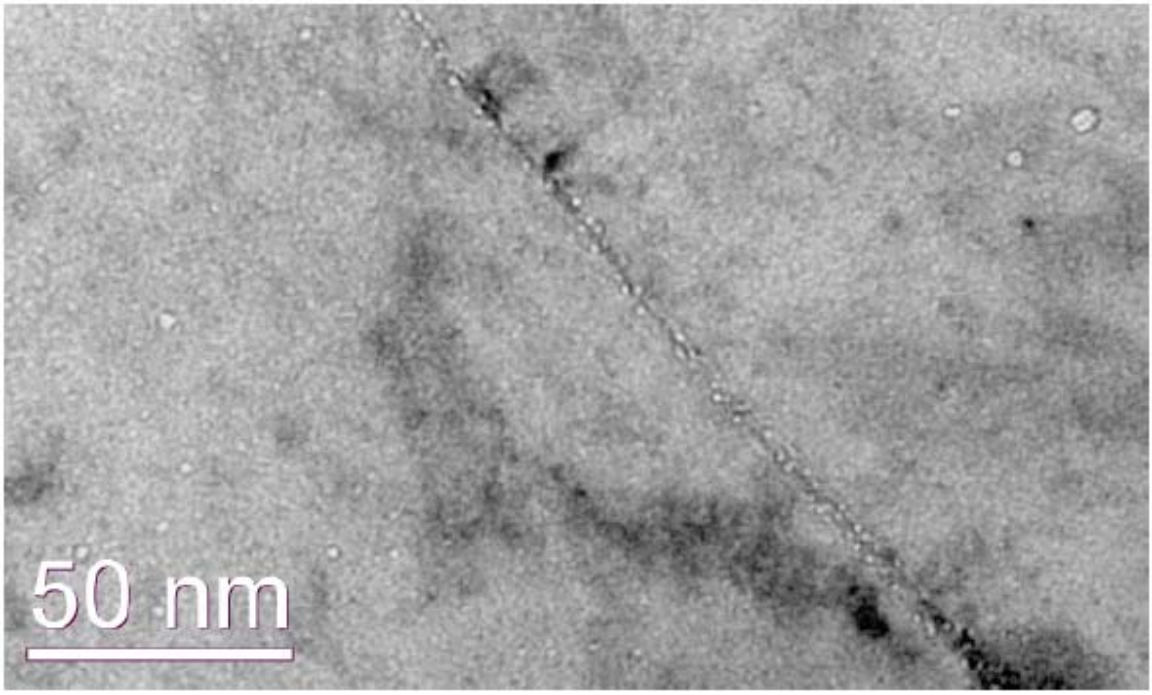

Figure 8: Grain boundary decorated with He bubbles in F82H at 500 C, 9 dpa and 190 He/dpa. From (xx)

Figure 8 shows the mechanism of property degradation by He bubble formation, namely a fine dispersion of bubbles at grain boundaries which promote intergranular or creep fracture. The lifetime under creep conditions is determined by the kinetics of bubble growth.

Incubation dose for swelling: After a dose of about 100 dpa, ferritic steels show a strong swelling rate of ~ 0.2 %/dpa, comparable to austenitic steels, as shown in Figure 9. The reasons for this incubation dose have been the subject of research for many years. The expectations for ODS is that this incubation does extends up to 200 dpa.

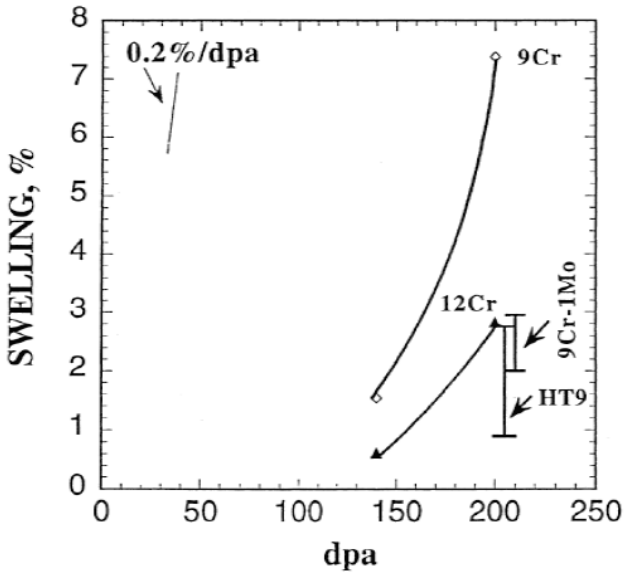

Figure 9: Swelling in ferritic steels shows a pronounced incubation effect that extends up to ~ 100 dpa. After that dose, swelling rate is as high as in austenitic steels. From (xx)

Design criterion #1, Strength: The temperature of operation of the FW in life, ~900 K, is at the upper limit of metals capabilities, as shown in Figure 10. However, the new ODS show enhanced strength of about 500 MPa at this temperature.

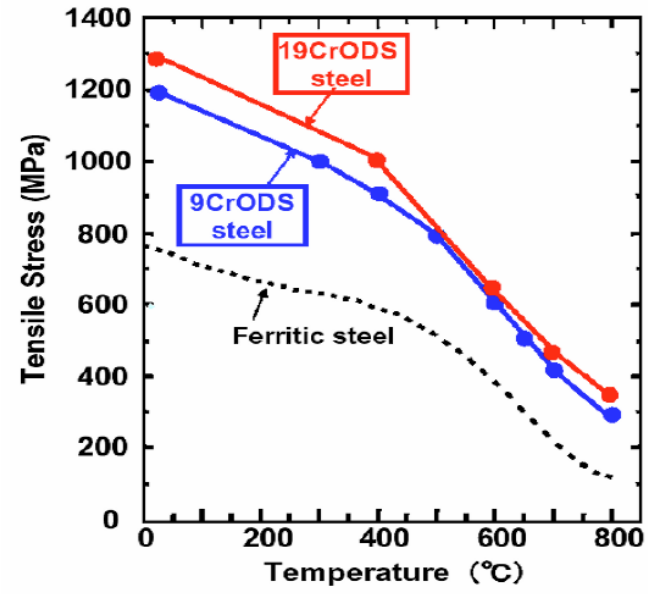

Figure 10: Strength of two ODS steels developed by A> Kimura, compared with traditional ferritic steels. From (77) .

Design criterion # 2 Corrosion resistance: In FeCR ferritic alloys, corrosion resistance and good ductility are mutually excluding properties. Corrosion resistance is strongly dependent on Cr content and manifests at Cr levels above ~ 9-10 at% Cr, see Figure 11, while α' precipitation, the cause of embrittlement, appears at the solubility limit that at the T's of interest for nuclear applications is above ~ 10 at% Cr. Therefore R&D has focused into the retardation of α' precipitation by means of alloying, giving a variety of chemical formulations from which we mention the work by A. Kimura in Japan, who obtained aging resistance by addition of 4% Al to alloys containing 14 – 22 at% Cr (77).

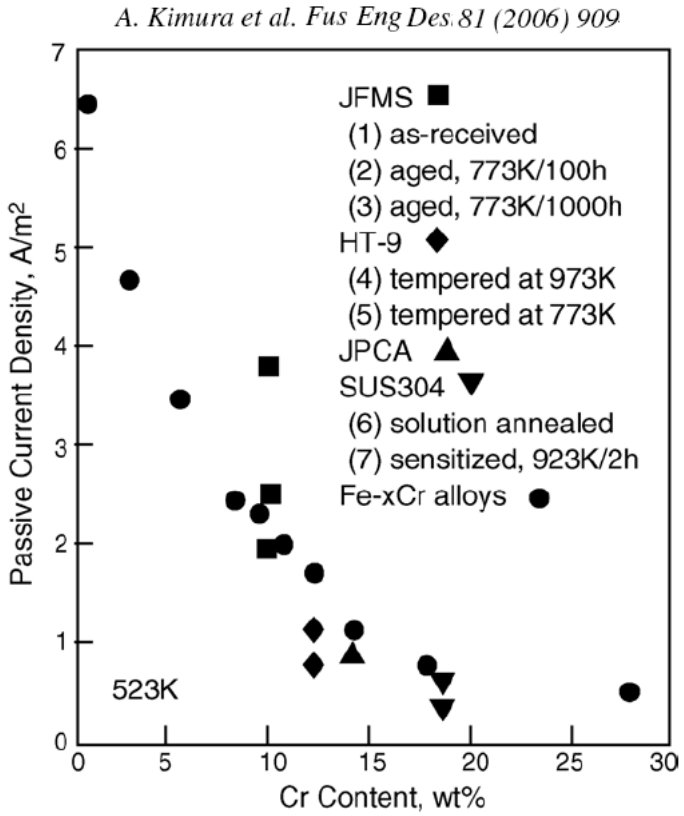

Figure 11: Corrosion rate of FeCr alloys as a function of Cr concentration. From (78).

Table I shows various formulations for the ODS alloys developed under the Japanese High Burnup Fuel Cladding Materials R&D program by A. Kimura et al. (77). These alloys are being irradiated at Japan and Russia to reach high dpa levels, and the results will be available for a few more years.

	Materials	Compositions	Alloys
K1	19Cr-ODS	19Cr+0.37Y_2O_3	Ferritic ODS steel
K2	14Cr-ODS	14Cr+4.5Al+0.38Y_2O_3	Ferritic ODS steel
K3	16Cr-ODS(2)	16Cr+4.5Al+0.37Y_2O_3	Ferritic ODS steel
K4	19Cr-ODS(3)	19Cr+4.5Al+0.37Y_2O_3	Ferritic ODS steel
K5	22Cr-ODS(3	22Cr+4.5Al+0.37Y_2O_3	Ferritic ODS steel

Table I: Composition of some ODS steels developed at Japan to provide high corrosion resistance and strength. From (77).

Design criterion # 3 Creep resistance: Creep resistance is probably the criterion that has more impact on the lifetime of the component. The Larson-Miller diagram shown in Figure 12 reports several ODS together with a conventional ferritic steel. For a life time of 10 years, or 100000 hs, at 1000 K the LMP parameter is 30000 and the corresponding stress that can be applied without failure is about 200 MPa. It is important to note that the black arrow on the plot indicates that the experiments were actually still running at the time of the publication, meaning that the actual value of the lifetime for every stress is larger than appearing in the plot, or in other words, the stress for 10 years is larger than 200 MPa. Many of the experimental results for this class of alloys are very recent or are still to be published in the future when radiations are finished.

Samples of mechanically alloyed (MA) MA957 ODS steel were irradiated in Fast Flux Test Facility (FFTF). This steel is of continued interest for nuclear applications. ODS-MA steels are known for their low swelling and embrittlement with exposure to high-energy neutrons (> 0.1 MeV) up to 10^{23} n/cm^2. MA956 (Fe-19Cr-0.33Ti-5Al-0.4Y-

0.15O-0.02C) has best high-temperature strength and oxidation resistance. ODS steel MA957 (Fe-14Cr-03.Mo-0.9Ti+0.25Y2O3) has similar properties. This steel is a 14Cr ferritic steel strengthened with a fine dispersion of ~5 nm yttrium oxide particles. Concerning irradiation creep, MA957 alloys have been shown to have better creep resistance than traditional F/M steels like HT9 above 550 C. ODS 12YWT (MA Fe-12Cr-3W-0.4Ti + Y2O3) alloy exhibits excellent high temperature creep strength superior to the other materials. It is not a commercial ODS steel, yet.

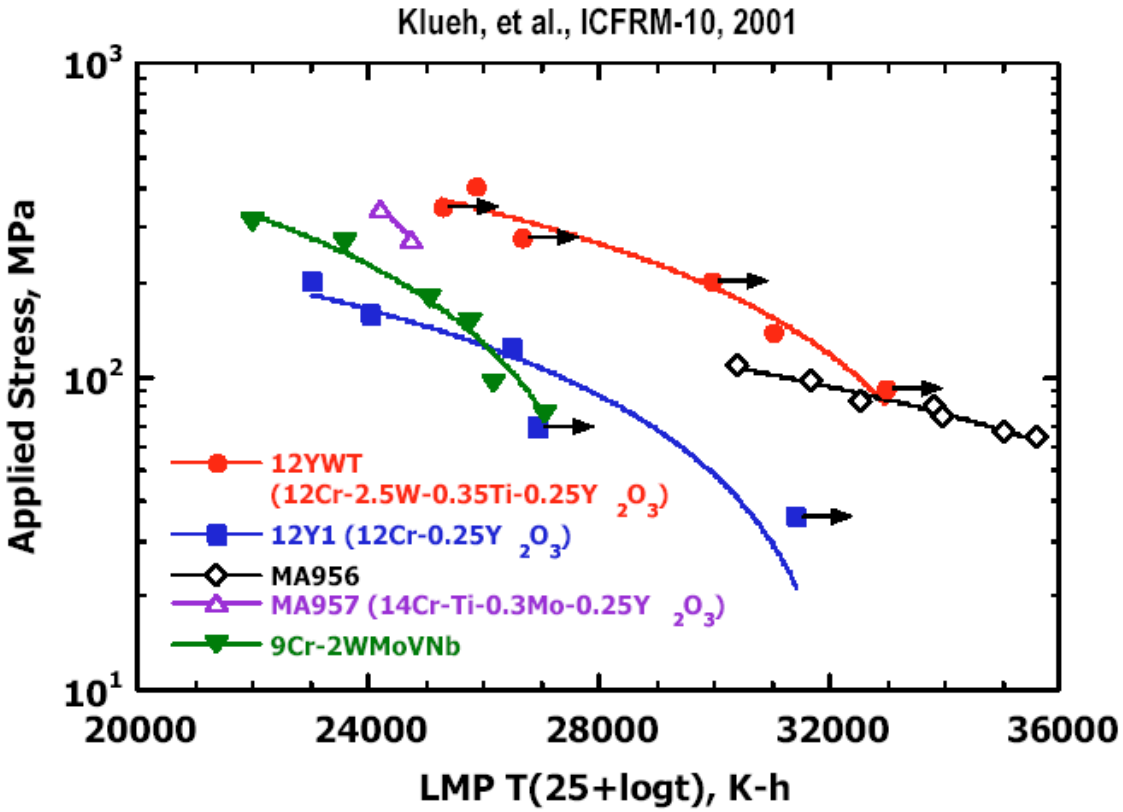

Figure 12: Larson Miller diagram for creep-rupture steenght of four ODS steels and a conventional ferritic/martensitic steel. Arrows indicate the tests are still running or it was discontinued before rupture. From (xx). Klueh et al. ICFRM-10, 2001.

There is a large amount of data reporting the achievements with ODS steels compared to the conventional ones. Figure 13 shows a factor of four increment in creep resistance for Japanese steels.

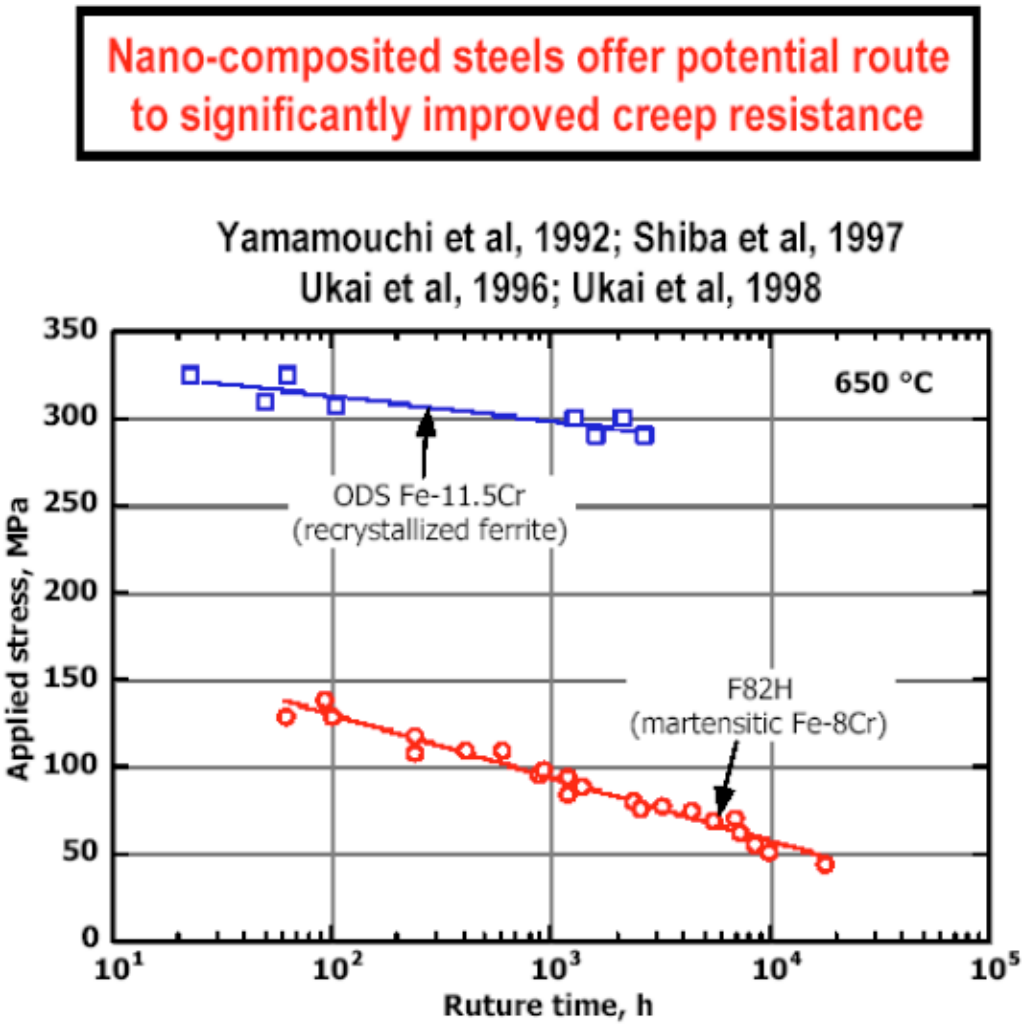

Figure 13: Nanocomposite steels offer a route to significantly improve creep resistance. From (79).

Design criterion # 6, dpa damage to the FW: From the strong energy dependence of the dpa cross section shown in Figure 8, we can analyze what part of the spectrum produces more damage. Figure 14 shows the percentiles of the spectrum and the damage at different energy cuts. Clearly the energetic neutrons (fast part of the spectrum are responsible for most of it. Similar to fast reactors, LIFE produces more damage per neutron than thermal reactors, and together with the higher He and H production discussed above, it makes radiation damage in LIFE the main concern from the materials perspective.

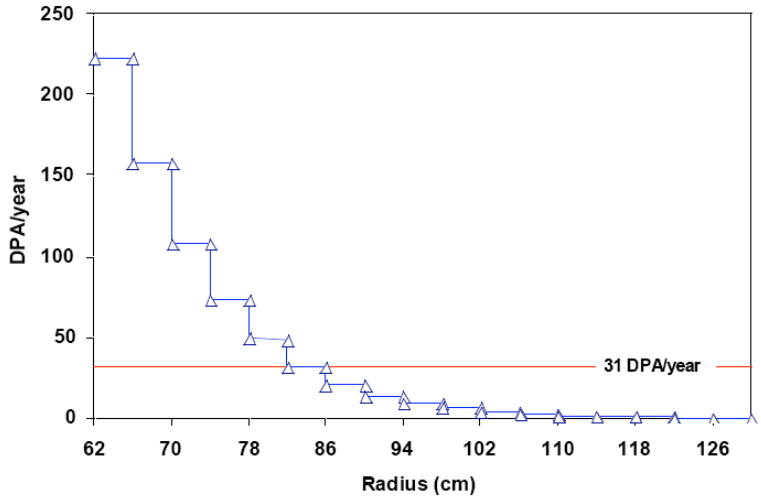

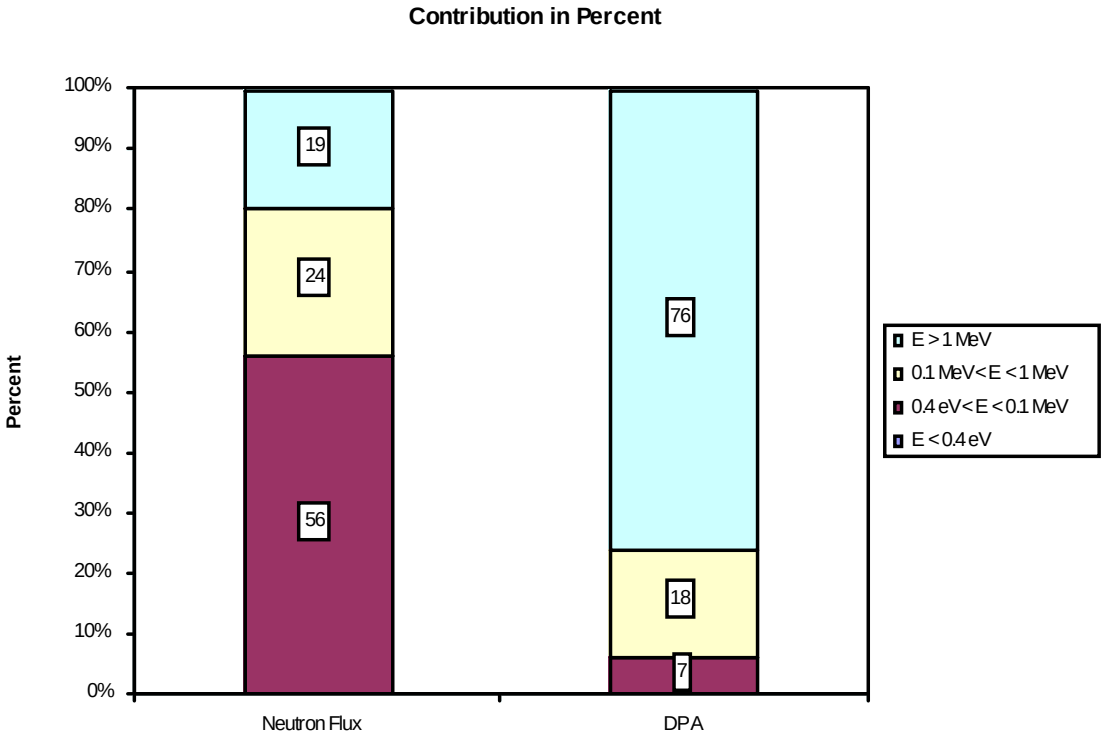

Figure 14: (upper figure) DPA damage rate as a function of position in the blanket for LIFE case xxx.(lower figure) Percentile contribution to damage for different neutron energy range in the spectrum. Clearly shown is the major impact of the fast component of the spectrum (E> 1 MeV) on the total damage. From M. Caro.

Ra

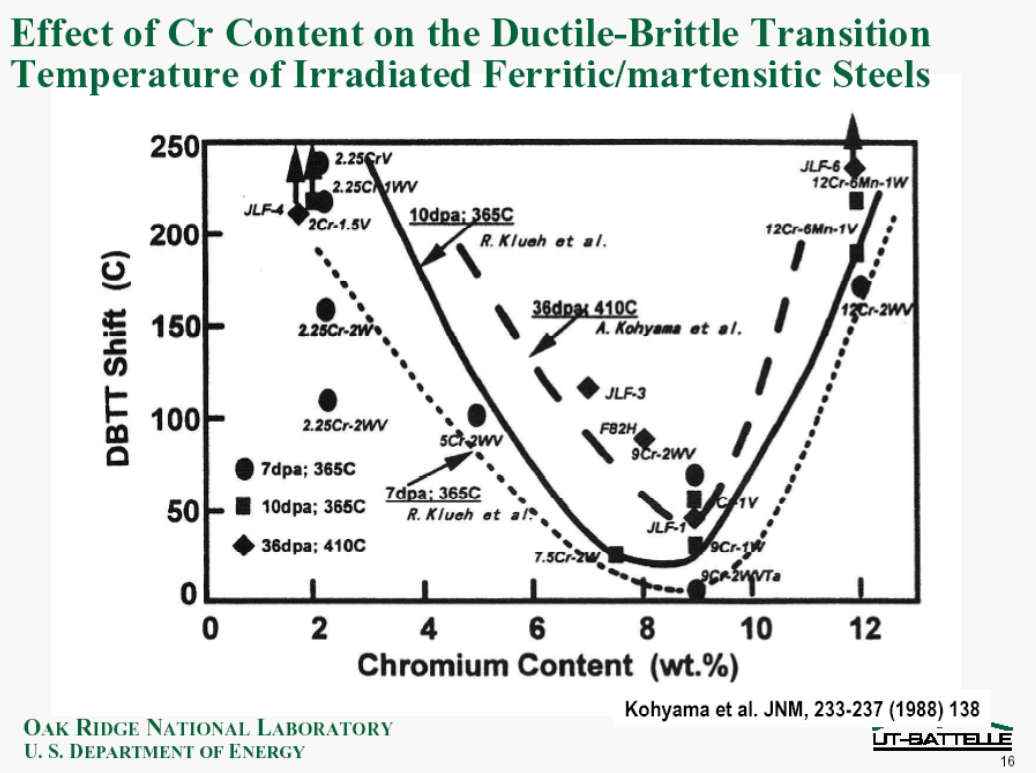

Figure 15: Ductile to brittle transition temperature, DBTT, shifts in FeCr steels versus Cr composition, at different levels of dpa damage. From Kohyama et al., 1988.

Design criteria # 4, Radiation induced embrittlement: Embrittlement of bcc ferritic steels is related to the increase in the ductile to brittle transition temperature, DBTT, induced by irradiation. In the development of FeCr alloys, it was early noticed that Cr composition plays an important role in embrittlement, as shown in Figure 15. For radiation levels between 7 and 36 dpa, the DBTT shift shows a pronounced minimum at ~ 9 % Cr. The physical origin of this minimum is a subject of intense research. As mentioned above the Cr composition of ferritic steels is a delicate balance between the corrosion resistance, which starts at x_Cr > ~ 10%, and the embrittlement resistance which requires it to be < ~ 10%. Several compositions are explored in different formulations of ODS ferritic steels, many of them with Cr content around 9 – 12 %.

Conclusions: The choice of ODS for the first wall in LIFE is the result of the significant world effort to develop these alloys and the impressive performance already achieved. In fact Japan and US has a leading role in developing composition and manufacturing processes to enhance a number of critical variables in particular an extremely high resistance to neutron irradiation. The ODS's can be candidates for structural materials because they have;1) high-temperature strength 2) high resistance to corrosion and 3) high resistance to neutron irradiation. Long-term aging embrittlement and anisotropy in the properties are also considered to be critical for these steels. Nano/mesostructure control enables the steels to meet the above requirements

CHAPTER C: Identification of Gaps in Knowledge & Vulnerabilities

From the preceding chapter, it is clear that the study of ferritic steels is a major research enterprise in most nuclear countries and consequently LIFE can benefit from the results obtained. The present state of the art in alloy development allows LIFE to take advantage of the situation and design a first wall based on the most advanced steels for nuclear applications.

However there are some particular needs in LIFE where there are gaps in the knowledge.

-First is the fact that at the first wall a hard (14 MeV) neutron spectrum is present, with a large He and H per dpa production rate. This feature, particular of fusion environments, is worsen in LIFE by the fact that the flux is pulsed, creating a dpa rate orders of magnitude larger than in magnetic fusion devices. The precise consequences of this characteristic are unknown.

- Second is the complex geometry of the first wall in LIFE that requires a careful study of manufacturing processes since welding of these steels is not advised. In fact, the most advanced application by JAEA is a cylindrical cladding tube of ~ 2m in length with stir welded caps that sit outside the high flux area of the reactor core. For LIFE a major challenge will be to design the first wall in such a way that the vessel could actually be manufactured.

- The third challenge comes from the fact that the damage dose that ODS steels can stand today is about 200 dpa, while the damage rate in LIFE's FW is ~ 40 dpa/year. It gives a lifetime of approximately 5 years. Since the cost of replacing the vessel is significant, a precise estimation of the lifetime is necessary for the accuracy of the cost model. From the issues raised in the first point above, it appears clear that it will be very difficult to predict the lifetime with accuracy.

CHAPTER D: Strategy and Future Work

Scope of an R&D program: Through inspection of the literature we have identified in Chapter B the main issues that R&D efforts around the world are focusing on. A number of general observations can be made:

- Every major country that has an R&D effort on ODS steels have come out with its own composition and thermo mechanical treatment. Depending on the type of reactor/coolant combination, corrosion is for some cases a major concern, which determines the composition of Cr on the main binary in the system, namely FeCr. High Cr content is beneficial for corrosion resistance but prejudicial for embrittlement, so additional alloying elements such as Al have to be added to prevent formation of α', the Cr-rich phase responsible for embrittlement. Similarly, the C content is adjusted to obtain the martensitic phase with its lath interfaces which contributes to hardness but limit ductility. In US there are several efforts, each focused in their own formulation for the alloy.

A combination of experimental and modeling activities are needed as part of the LIFE R&D effort on first wall to better understand the radiation-induced processes occurring in service and to help deriving better limits of operating conditions based on integrity and lifetime requirements. Research on He management via nanostructuring is the path followed by other research groups. The parameter space for thermo-mechanical treatments is so large that we can safely say that the best nano-microstructure is still to be found.

The experimental program under construction for LIFE should involve ion and neutron irradiations, He implantation and retention, studies of fatigue in the ferritic-steel/W bond. The range of testing facilities should allow for the isolation of specific processes to help in understanding the governing mechanisms.

It seems wise to develop collaborations, in particular with Japan and US producers of ODS steels to work on our own LIFE issues but on their alloys, so we can take advantage of the large body of research and characterization already published for those particular compositions.

In conclusion this report has reviewed the major first wall issues and has identified the design window and the lifetime limiting factors. We arrived at the conclusion that a first wall made of ODS ferritic steel may have a lifetime long enough to achieve deep burn up of Pu based fuel, while for SNF or DU fuels, replacement of the chamber every ~five years must be envisaged. More precise lifetime evaluations require the specific neutron flux and fluence for each particular case.

Finally, the world interest on these new type of alloys is so large, that moving the frontier forward, well above 200 dpa's, is to be expected soon as basic science based on computational materials modeling in combination with careful experimental validation may accelerate the optimization of alloys in ways never foreseen before.

LIFE requirements are daunting, but not impossible, challenges. Such challenges underscore the need for advanced physical models of alloy thermokinetics and nano-microstructural evolutions during both processing-fabrication sequences and under long-term service, as well as integrated predictive models of mechanical properties. Such models are being developed, at LLNL and elsewhere, to guide alloy design and optimization as well as to predict structural performance and lifetime limits.

Bibliography

1. G. R. Odette, M. J. Alinger, and B. D. Wirth. Recent developments in irradiation resistant steels. Annu. Rev. Mater. Res. 38, 20.1 (2008)

A. Kohyama, A. Hishinuma, D.S. Gelles, R.L. Klueh, W. Dietz, K. Ehrlich. Jr. Nuc. Mat. 233, 138 (1988).

2. Lee EH, Mansur LK. 1990. Mechanisms of swelling suppression in cold-worked phosphorus-modified Fe-Ni-Cr alloys. Philos. Mag. A 61:733–49

3. Maziasz PJ. 1993. Overview of microstructural evolution in neutron-irradiated austenitic stainless-steels. J. Nucl. Mater. 205:118–45

4. Ukai S, Uwaba T. 2003. Swelling rate versus swelling correlation in 20% cold-worked 316 stainless steels. J. Nucl. Mater. 317:93–101

5. Kimura A, Kasada R, Morishita K Sugano R, Hasegawa A, et al. 2002. High resistance to helium embrittlement in reduced activation martensitic steels. J. Nucl. Mater. 307:521–26

6. Klueh RL, Nelson AT. 2007. Ferritic/martensitic steels for next-generation reactors. J. Nucl. Mater. 371:37–52

7. Klueh RL, Hashimoto N, Maziasz PJ. 2007. New nano-particle strengthened ferritic/martensitic steels by conventional thermo-mechanical treatment. J. Nucl. Mater. 367–370:48–53

8. Fisher JJ. 1978. Dispersion strengthened ferritic alloy for use in liquid-metal fast breeder reactors. U.S. Patent No. 4,075,010

9. Kasada R, Toda N, Yutani K, Cho HS, Kishimoto H, Kimura A. 2007. Pre- and post-deformation microstructures of oxide dispersion strengthened ferritic steels. J. Nucl. Mater. 367–370:222–28

10. Hamilton ML, Gelles DS, Lobsinger RJ, Johnson GD, Brown WF, et al. 2000. Fabrication technological development of the oxide dispersion strengthened alloy MA957 for fast reactor applications. PNL-13168, Richland,WA: Pac. Northwest Lab.

11. Ukai S, Ohtsuka S. 2007. Nano-mesoscopic structure control in 9Cr-ODS ferritic steels. Energy Mater. 2:26–35

79. Ukai S, Nishida T, Okuda T, Yoshitake T. 1998. R&D of oxide dispersion strengthened ferritic martensitic steels for FBR. J. Nucl. Mater. 258–263:1745–49

12. Ohta J, Ohmura T, Kako K, Tokiwai M, Suzuki T. 1995. Hardness of 12Cr-8Mo ferritic steels irradiated by Ni ions. J. Nucl. Mater. 225:187–91

13. Saito J, Suda T, Yamashita S, Ohnuki S, Takahashi H, et al. 1998. Void formation and microstructural development in oxide dispersion strengthened ferritic steels during electron irradiation. J. Nucl. Mater. 258–263:1264–68

14. Kuwabara T, Kurishita H, Ukai S, Narui M, Mizuta S, et al. 1998. Superior Charpy impact properties of ODS ferritic steel irradiated in JOYO. J. Nucl. Mater. 258–263:1236–41

15. Yamashita S, Watanabe S, Ohnuki S, Takahashi H, Akasaka N, Ukai S. 2000. Effect of mechanical alloying parameters on irradiation damage in oxide dispersion strengthened ferritic steels. J. Nucl. Mater. 283–287:647–51

16. Akasaka N, Yamashita S, Yoshitake T, Ukai S, Kimura A. 2004. Microstructural changes of neutron irradiated ODS ferritic and martensitic steels. J. Nucl. Mater. 329–333:1053–56

17. Yamashita S, Oka K, Ohnuki S, Akasaka N, Ukai S. 2002. Phase stability of oxide dispersion strengthened ferritic steels in neutron irradiation. J. Nucl. Mater. 307–311:283–88

18. Yamashita S, Akasaka N, Ohnuki S. 2004. Nano-oxide particle stability of 9–12Cr grain morphology modified ODS steels under neutron irradiation. J. Nucl. Mater. 329–333:377–81

19. Yoshitake T, Abe Y, Akasaka N, Ohtsuka S, Ukai S, Kimura A. 2004. Ring-tensile properties of irradiated oxide dispersion strengthened ferritic/martensitic steel claddings. J. Nucl. Mater. 329–333:342–46

20. Yamashita S, Oka K, Yoshitake T, Akasaka N, Ukai S, Ohnuki S. 2004. Oxide particle stability in oxide dispersion strengthened ferritic steels during neutron irradiation. Int. Symp. Eff. Radiat. Mater., 21st, Tucson, ASTM Spec. Top. Publ. 1447:391. Philadelphia: ASTM

21. Yamashita S, Yoshitake T, Akasaka N, Ukai S, Kimura A. 2005. Mechanical behavior of oxide dispersion strengthened steels irradiated in JOYO. Mater. Trans. 46:493–97

22. Kishimoto H, Yutani K, Kasada R, Kimura A. 2006. Helium cavity formation research on oxide dispersion strengthening (ODS) ferritic steels utilizing dual-ion irradiation facility. Fus. Eng. Des. 81:1045–49

23. Kishimoto H, Yutani K, Kasada R, Hashitomi O, Kimura A. 2007. Heavy-ion irradiation effects on the morphology of complex oxide particles in oxide dispersion strengthened ferritic steels. J. Nucl. Mater. 367–370:179–84

24. Cho HS, Kasada R, Kimura A. 2007. Effects of neutron irradiation on the tensile properties of high-Cr oxide dispersion strengthened ferritic steels. J. Nucl. Mater. 367–370:239–43

25. Yamashita S, Akasaka N, Ukai S, Ohnuki S. 2007. Microstructural development of a heavily neutronirradiated ODS ferritic steel (MA957) at elevated temperature. J. Nucl. Mater. 367–370:202–7

26. Yutani K, Kishimoto H, Kasada R, Kimura A. 2007. Evaluation of helium effects on swelling behavior of oxide dispersion strengthened ferritic steels under ion irradiation. J. Nucl. Mater. 367–370:423–27

27. Kimura A, Cho HS, Toda N, Kasada R, Utani K, et al. 2007. High burnup fuel cladding materials R&D for advanced nuclear systems: nano-sized oxide dispersion strengthening steels. J. Nucl. Sci. Technol. 44:323–28

28. Chou TS, Bhadeshia HKDH. 1993. Crystallographic texture in mechanically alloyed oxide-dispersionstrengthened MA956 and MA957 steels. Metall. Trans. A 24A:773–79

29. Capdevila C, Bhadeshia HKDH. 2001. Manufacturing and microstructural evolution of mechanically alloyed oxide dispersion strengthened superalloys. Adv. Eng. Mater. 3:647–56

30. Chen YL, Jones AR, Miller U. 2002. Origin of porosity in oxide-dispersion-strengthened alloys produced by mechanical alloying. Metall. Mater. Trans. A 33A:2713–18

31. Alamo A, Lambard V, Averty X, Mathon MH. 2004. Assessment of ODS-14%Cr ferritic alloy for high temperature applications. J. Nucl. Mater. 329–333:333–37

32. Wilshire B, Lieu TD. 2004. Deformation and damage processes during creep of Incoloy MA957. Mater. Sci. Eng. A386:81–90

33. Alamo A, Bertin JL, Shamardin VK, Wident P. 2007. Mechanical properties of 9Cr martensitic steels and ODS-FeCr alloys after neutron irradiation at 325◦C up to 42 dpa. J. Nucl. Mater. 367–370:54–59

34. Lindau R, Moslang A, Schirra M, Schlossmacher P, Klimenkov M. 2002. Mechanical and microstructural properties of a hipped RAFM ODS-steel. J. Nucl. Mater. 307–311:769–72

35. Schaeublin R, Leguey T, Spatig P, Baluc N, Victoria M. 2002. Microstructure and mechanical properties of two ODS ferritic/martensitic steels. J. Nucl. Mater. 307–311:778–82

36. Lucon E. 2002. Mechanical tests on two batches of oxide dispersion strengthened RAFM steel (Eurofer97). Fus. Eng. Des. 61–62:683–89

37. Klimiankou M, Lindau R, Moslang A. 2003. HRTEM study of yttrium oxide particles in ODS steels for fusion reactor application. J. Cryst. Growth 249:381–87

38. Cayron C, Rath E, Chu I, Launois S. 2004. Microstructural evolution of Y2O3 and MgAl2O4 ODS EUROFER steels during their elaboration by mechanical milling and hot isostatic pressing. J. Nucl. Mater. 335:83–102

39. Monnet I, Dubuisson P, Serruys Y, Ruault MO, Kaitasov O, Jouffrey B. 2004. Microstructural investigation of the stability under irradiation of oxide dispersion strengthened ferritic steels. J. Nucl. Mater. 335:311–21

40. Klimiankou M, Lindau R, Moslang A. 2004. TEM characterization of structure and composition of nanosized ODS particles in reduced activation ferritic-martensitic steels. J. Nucl. Mater. 329–333:347–51

41. Lindau R, Moslang A, Rieth M, Klimiankou M, Materna-Morris E, et al. 2005. Present development status of EUROFER and ODS-EUROFER for application in blanket concepts. Fus. Eng. Des. 75– 79:989–96

42. Klimiankou M, Lindau R, Moslang A. 2005. Energy-filtered TEM imaging and EELS study of ODS particles and argon-filled cavities in ferritic-martensitic steels. Micron 36:1–8

43. Yu G, Nita N, Baluc N. 2005. Thermal creep behaviour of the Eurofer97 RAFM steel and the two European ODS Eurofer97 steels. Fus. Eng. Des. 75–79:1037–41

44. Mathon M, Carlan Y, Averty X, Alamo A, Novion CH. 2005. Small angle neutron scattering study of irradiated martensitic steels: relation between microstructural evolution and hardening. J. ASTM Int. 2:120–34

45. Klimiankou M, Lindau R, Moslang A. 2007. Direct correlation between morphology of (Fe,Cr)23C6 precipitates and impact behavior of ODS steels. J. Nucl. Mater. 367–370:173–78

46. Oksiuta Z, Baluc N. 2008. Microstructure and Charpy impact properties of 12–14Cr oxide-dispersion strengthened steels. J. Nucl. Mater. 374:178–84

47. Romanoski GR, Snead LL, Klueh RL, Hoelzer DT. 2000. Development of an oxide dispersion strengthened, reduced-activation steel for fusion energy. J. Nucl. Mater. 283–287:642–46

48. Larson DJ, Maziasz PJ, Kim IS, Miyahara K. 2001. Three-dimensional atom probe observation of nanoscale titanium-oxygen clustering in an oxide-dispersion-strengthened Fe-12Cr-3W-0.4Ti + Y2O3 ferritic alloy. Scr. Mater. 44:359–64

49. Klueh RL, Maziasz PJ, Kim IS, Heatherley L, Hoelzer DT, et al. 2002. Tensile and creep properties of an oxide dispersion-strengthened ferritic steel. J. Nucl. Mater. 307–311:773–77

50. Alinger MJ, Odette GR, Lucas GE. 2002. Tensile and fracture toughness properties of MA957: implications to the development of nanocomposited ferritic alloys. J. Nucl. Mater. 307–311:484–89

51. Miller MK, Kenik EA, Russell KF, Heatherley L, Hoelzer DT, Maziasz PJ. 2003. Atom probe tomography of nanoscale particles in ODS ferritic alloys. Mater. Sci. Eng. A 353:140–45

52. Kim IS, Choi BY, Kang CY, Okuda T, Maziasz PJ, Miyahara K. 2003. Effect of Ti and W on the mechanical properties and microstructure of 12% Cr base mechanical-alloyed nano-sized ODS ferritic alloys. ISIJ Int. 43:1640–46

53. Alinger MJ, Odette GR, Hoezler DT. 2004. The development and stability of Y-Ti-O nanoclusters in mechanically alloyed Fe-Cr based ferritic alloys. J. Nucl. Mater. 329–333:382–86

54. MillerMK,HoelzerDT,Kenik EA, Russell KF. 2004. Nanometer scale precipitation in ferriticMA/ODS alloy MA957. J. Nucl. Mater. 329–333:338–41

55. Alinger MJ. 2004. On the formation and stability of nanometer scale precipitates in ferritic alloys during processing and high temperature service. PhD thesis. Univ. Calif., Santa Barbara. 341 pp.

56. Kishimoto H, Alinger MJ, Odette GR, Yamamoto T. 2004. TEM examination of microstructural evolution during processing of 14CrYWTi nanostructured ferritic alloys. J. Nucl. Mater. 329–333:369–71

57. Alinger MJ, Odette GR. 2005. On the precipitation kinetics, thermal stability and strengthening mechanisms of nanometer scale Y-Ti-O clusters in nanostructured ferritic alloys. Fusion Mater. Semiannu. Prog. Rep. DOE-ER-03 13/37 61–69, DOE, Oak Ridge, TN

58. Alinger MJ, Odette GR, Hoelzer DT. 2008. On the role of alloy composition and processing variables in nanofeature formation and dispersion strengthening in nanostructured ferritic alloys. Fusion Mater. Semiannu. Prog. Rep. DOE-ER-0313/43, DOE, Oak Ridge, TN

59. Klueh RL, Shingledecker JP, Swindeman RW, Hoelzer DT. 2005. Oxide dispersion-strengthened steels: a comparison of some commercial and experimental alloys. J. Nucl. Mater. 341:103–14

60. Miller MK, Hoelzer DT, Kenik EA, Russell KF. 2005. Stability of ferritic MA/ODS alloys at high temperatures. Intermetallics 13:387–92

61. Miller MK, Russell KF, Hoelzer DT. 2006. Characterization of precipitates in MA/ODS ferritic alloys. J. Nucl. Mater. 351:261–68

62. Sokolov MA,Hoelzer DT, Stoller RE, McClintock DA. 2007. Fracture toughness and tensile properties of nano-structured ferritic steel 12YWT. J. Nucl. Mater. 367–370:213–16

63. Miao P, Odette GR, Yamamoto T, Alinger MJ, Hoelzer D, Gragg D. 2007. Effects of consolidation temperature, strength, and microstructure on fracture toughness of nanostructured ferritic alloys. J. Nucl. Mater. 367–370:208–12

64. Miao P, Odette GR, Yamamoto T, Alinger MJ, Klingensmith D. 2008. Thermal stability of nanostructured ferritic alloys. J. Nucl. Mater. In press

65. Yang WJ, Odette GR,Yamamoto T, Miao P, Alinger MJ, et al. 2007.Acritical stress-critical area statistical model of the KJc(T) curve for MA957 in the cleavage transition. J. Nucl. Mater. 367–370:616–20

66. Hoelzer DT, Bentley J, Sokolov MA, Miller MK, Odette GR, Alinger MJ. 2007. Influence of particle dispersions on the high-temperature strength of ferritic alloys. J. Nucl. Mater. 367–370:166–72

67. Miao P, Odette GR, Gould J, Bernath J, Miller R, et al. 2007. The microstructure and strength properties of MA957 nanostructured ferritic alloy joints produced by friction stir and electro-spark deposition welding. J. Nucl. Mater. 367–370:1197–1202

68. Gelles DS. 1996. Microstructural examination of commercial ferritic alloys at 200 dpa. J. Nucl. Mater. 233–237:293–98

69. Tolozcko MB, Garner FA, Eiholzer CR. 1998. Irradiation creep of various ferritic alloys irradiated at 400◦C in the PFR and FFTF reactors. J. Nucl. Mater. 258–263:1163–66

70. Kim IS, Hunn JD, Hashimoto N, Larson DL, Maziasz, et al. 2000. Defect and void evolution in oxide dispersion strengthened ferritic steels under 3.2 MeV Fe+ ion irradiation with simultaneous helium injection. J. Nucl. Mater. 280:264–74

71. Tolozcko MB, Gelles DS, Garner FA, Kurtz RJ, Abe K. 2004. Irradiation creep and swelling from 400 to 600◦C of the oxide dispersion strengthened ferritic alloy MA957. J. Nucl. Mater. 329–333:352–55

72. Allen TR, Gan J, Cole JI, Ukai S, Shutthanandan V, Thevuthasan S. 2005. The stability of 9Cr-ODS oxide particles under heavy-ion irradiation. J. Nucl. Sci. Eng. 151:305–12

73. Yamamoto T, Odette GR, Miao P, Hoelzer DT, Bentley J, et al. 2007. The transport and fate of helium in nanostructured ferritic alloys at fusion relevant He/dpa ratios and dpa rates. J. Nucl. Mater. 367–370:399–410

74. Rieth M, Schirra M, Falkenstein A, Graf P, Heger S, et al. 2003. Eurofer97 tensile, charpy, creep, and structural tests. Forsch. Karlsruhe FZKA6911

75 S. Zinkle and N. Ghoniem, Fusion Engr. Des. 51, 55 (2000).

76. M. B. Toloczko and F. A. Garner. Jr. Nuc. Mat. 233, 289 (1996).

77. A. Kimura, H. S. Cho, N. Toda et al. High burnup fuel cladding materials R&D for water-cooling nuclear power plants. Jr. Nuc. Sci. and Tech. 44, 323 (2007).

78. Gosta Wranglen, Introduction to corrosion and protection of metals. Chapman and Hall, New York (1985).

79. Odette GR. 1988. On mechanisms controlling swelling in ferritic and martensitic alloys. J. Nucl. Mater. 155–157:921–27